ACADEMIA ROMÂNĂ
Revue Roumaine de Chimie
https://www.icf.ro/rrch/

Rev. Roum. Chim.,
2025, *70*(1–2), 5–23
DOI: 10.33224/rrch.2025.70.1-2.01

Papers

A NOVEL COLORIMETRIC NAKED EYE DETECTION PROBE FOR M^{2+} AND M^{3+} IONS BASED ON A N,O-DONOR LIGAND: SYNTHESIS, CHARACTERIZATION AND CATALYTIC PROPERTIES

Djouhra AGGOUN,[*,a,b] Salima TABTI,[c] Raúl BERENGUER,[d] Emilia MORALLÓN[d] and Ali OURARI[a]

[a] Laboratory of Electrochemistry, Molecular Engineering and Redox Catalysis (LEIMCR), Faculty of Technology, Ferhat ABBAS University of Sétif-1, Sétif 19000, Algeria
[b] Department of Chemistry, Faculty of Science, Ferhat ABBAS University of Sétif-1, Sétif 19000, Algeria
[c] Department of Ecology and Environment, Faculty of Life and Natural Sciences of Earth and Univers Sciences, University Mohamed El Bachir El Ibrahimi of Bordj Bou Arreridj, 34000, Algeria
[d] Department of Physical Chemistry, University Institute of Materials, University of Alicante, Ap.99, 03080 Alicante, Spain

Received August 10, 2023

A novel N,O-donor ligand (HL) type Schiff base was synthesized and was then used to synthesize a new copper complex. Both the ligand and the complex were characterized by elemental analysis and FT-IR, ^{1}HNMR, XPS and UV-Vis. spectroscopies to elucidate their chemical compositions and structures. Results evidenced the synthesis of a $Cu(L)_2{\cdot}2H_2O$ complex based on coordinate bonds between Cu(II) and N/O heteroatoms. Furthermore, the thermal and electrochemical properties were studied by thermogravimetry and cyclic voltammetry, respectively. The quasi-reversible Cu(II)/Cu(I) and Cu(III)/Cu(II) processes observed by cyclic voltammetry evidenced the electrochemical activity of this new complex, thus, exhibiting potential interest for electrochemical applications in organic media. On the other hand, the ability of the ligand for complexing M^{2+} and M^{3+} ions was investigated by colorimetric and UV-Vis. measurements. Results suggest that this novel ligand was found to be highly selective and sensitive for the recognition of Cu^{2+} and Co^{2+} or Fe^{2+} and Fe^{3+} ions in acetonitrile or methanol solutions, demonstrating its potential interest to be used as naked-eye chemosensor of metal ions. The oxidation of a wide range of *o*-diphenols to *o*-quinones is catalyzed by the catechol oxidases. Therefore, to understand more about this biological process, the ability of the prepared ligand to contribute with other metals miming bio-organism puzzles has been also examined. So, distinct copper complexes prepared *in situ* by using five different copper salts $Cu(X)_y{\cdot}nH_2O$ ($X = NO_3^-$, Br^-, SO_4^{2-}, Cl^- and CH_3COO^-), three different ligand-to-metal ion ratios (L/M: 1/1, 2/1 or 1/2) and three different media (DMF, MeOH and ACN) were used to evaluate the catechol oxidation activity of the new ligand Cu-based complexes. The results show that the nitrate and bromide complexes in methanol solution with a L/M: 1/1 ratio exhibit the highest catecholase activity.

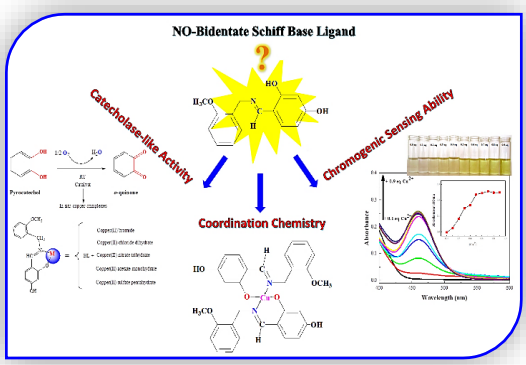

INTRODUCTION

Owing to their large structural versatility, Schiff base ligands containing oxygen and nitrogen as donor heteroatoms have been implicated in extensive research during the last years.[1,2] This kind of ligands seems to be very important as new class of chelating agents in coordination chemistry, since

[*] Corresponding author: aggoun81@yahoo.fr; djouhra.aggoun@univ-setif.dz

by a judicious selection of appropriate amine and aromatic ring substituents in precursors, they can act as modulators of structural and electronic properties of transition metals.[5]

Because of such versatility, polydentate Schiff bases ligands and/or their metal complexes present considerable interest in different areas and applications. Thus, these compounds can exhibit unique structural features[6] and catalytic properties,[7,8] for example, for organic transformations when the suitable ligands are associated to an appropriate metallic center.[9] In addition, these ligands and/or their complexes show potential interest, such as therapeutic agents, in a wide variety of biochemical processes,[10] and are attractive for several applications as antifungal,[11] antibacterial,[12] anticancer,[13] anticorrosion[14] agents, for electroanalysis[15] bio-sensoring,[16] etc.

On the other hand, the unique structural properties of polydentate Schiff bases ligands are of great interest for colorimetric chemosensors of metallic ions, since their detection can be "naked-eye" attained based on their right combination of a suitable receptor and chromophore. Thus, these ligands can show different and/or variable colorimetric (optical) responses with metal ions, acting as molecular chemosensors. Among different approaches in literature, naked-eye detection methods offer several advantages and have received immense attention, since they offer qualitative and quantitative information in a facile, cost-effective and real time-monitoring (rapid) manner.[17]

Furthermore, an extensive literature search revealed that the majority of Schiff-ligand complexes with d-block transition metals can contribute as catalysts in several catalytic and electrocatalytic processes.[18,19] Particularly, t is well known that Ru(III), Co(II) and Mn(III) complexes have been used as catalyst for alkene epoxidation.[20] In order to produce of novel medications or compounds, these complexes have also a significant interest in pharmaceutical and biochemistry because of their varied biological activities. Thus, the most described biological activities are antitumoral, antimicrobial, antioxidant, DNA-binding, antidiabetic, antimalarial, catalase-like and catecholase-like enzymatic.[21] Remarkably, copper complexes of Schiff bases have garnered great attention in these areas. This specie plays relevant roles in several metabolic functions of humans[22] and it is one of the main reasons encouraging the chemical processes such as those of catalytic or electrocatalytic oxidations.[23] The copper complexes of bidentates Schiff bases readily yield stable and intense colored metal complexes which have been showed and exhibited interesting physical and chemical properties.[24]

Recently, great deal of attention has been received to these synthetic compounds that can activate molecular oxygen because of their aptitude to oxidize organic molecules which are essentially important to life. Catecholase is the most crucial metalloprotein that catalyze the oxidation reactions of catechols to their corresponding o-quinones coupled with the $2e^-/2H^+$ reduction of oxygen to water which are very reactive compounds. As consequence, they can produce melanin by auto-polymerization which may defend tissues from the damages caused by pathogens and insects. So, in view of the countless rank of oxidation reactions, many biomimetic compounds with synthetic procedures have been reported to yield new and effective oxidation catalysts that exhibit catecholase activities.[25,26] Also, the goal to use combination L/Cu^{II}(salt) as catalyst is the miming the active sites of the type 3 copper proteins/enzymes such as hemocyanin, tyrosinase and catechol oxidase.

Due to the potential interest of these compounds, this research work studies the synthesis and main properties of a novel N,O-bidentate Schiff base ligand and its copper complex. Both the ligand and the complex have been thoroughly characterized by some of the most powerful analytical techniques to investigate their chemical composition and structure, as well as their main thermal, optical, electrochemical and catalytic properties. Thus, as a continuation to our recent contributions,[27] the present work aims to explore the potential implications of bidentate Schiff base ligands in important areas, like molecular chemosensors or various electrochemical and catalytic applications.

EXPERIMENTAL

1. Chemicals

All chemicals were obtained from commercial sources and were used as received without any further purification. All solvents, namely, methanol (MeOH), acetonitrile (ACN), tetrahydrofuran (THF), dimethylformamide (DMF), dimethylsulfoxide (DMSO) and methylenechloride (DCM), were obtained from Fluka, whereas (2-Methoxyphenyl) methanamine 99% and β-Resorcylaldehyde 99% were from Sigma Aldrich.

2. Synthesis of the ligand and its copper complex

For the synthesis of the bidentate Schiff base ligand (HL) (Scheme 1), 1 mmol (138 mg) of β-Resorcylaldehyde and 1 mmol (137 mg) of (2-Methoxyphenyl) methanamine were added to a 250 mL round bottom flask containing 10 mL of absolute methanol. The contents were refluxed for 2 h under stirring to render the condensation reaction. After evaporating the solvent, the formed yellow precipitate was collected and washed with small portions of diethylether. Finally, 230 mg of the ligand were obtained, being the yield 90%.

To prepare the novel bis-bidentate Schiff base copper complex $[Cu(L)_2{\cdot}2H_2O]$ (Scheme 1), the HL ligand (514 mg, 5 ml MeOH) was contacted with copper acetate monohydrate (Metal precursor: 199 mg, 10 ml MeOH) in 2:1 molar ratio. The reaction was carried out under reflux for 4 h. Then, the solvent was eliminated under reduced pressure and the resulting solid was recovered by filtration. Finally, the desired compound was easily leached by washing the solid with small portions of diethylether yielding 75% of olive powder complex.

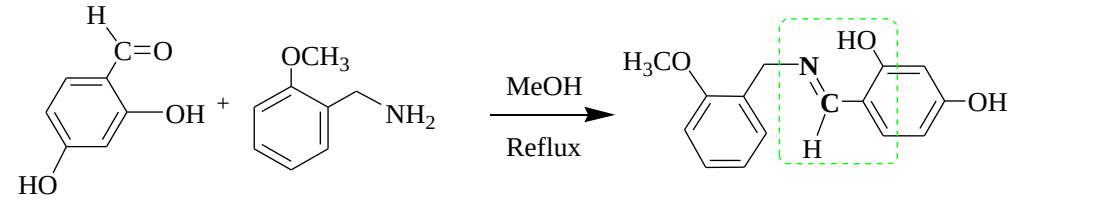

B-Resorcylaldehyde (2-Methoxyphenyl)methanamine 4-[(2-Methoxy-benzylimino)-methyl]-benzene-1,3-diol

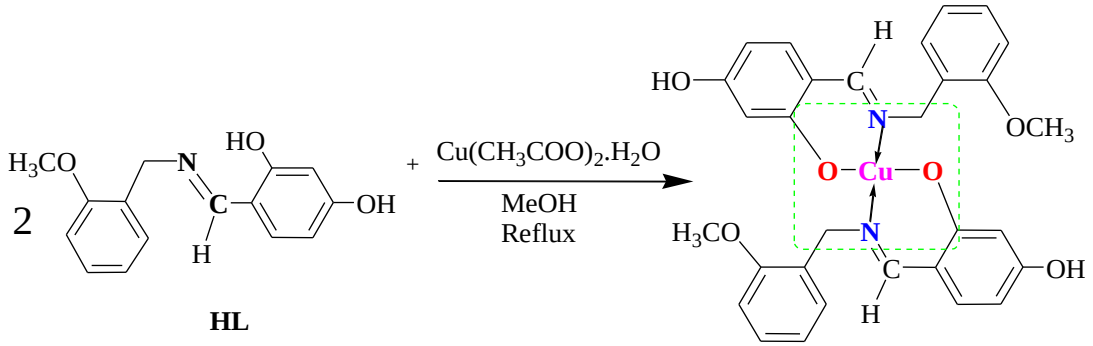

HL **$Cu^{II}(L)_2{\cdot}2H_2O$**

Scheme 1 – Schematic illustration of the synthesis and chemical structure of HL and its copper complex $[Cu^{II}(L)_2{\cdot}2H_2O]$.

3. Physico-chemical and electrochemical characterization

The obtained new compounds were characterized by elemental analysis with a vario EL III elemental analyzer by using a (C, N, H) LECO analyzer (Micro TruSpec model). This analysis was repeated three times to confirm the reproducibility of the results. FT-IR spectra were recorded on a Perkin Elmer 1000-FTIR Spectrometer using KBr disks, while the electronic spectra (UV-Vis.) were obtained on a Unicam UV-300 Spectrophotometer having 1 cm as path length cell. The ^{1}HNMR spectrum was recorded on a Bruker AC300 Y 400 at room temperature using deuterated DMSO-d_6 as solvent and the chemical shifts (δ), expressed in ppm, were referenced to tetramethylsilane (TMS) used as internal reference. The X-ray photoelectron spectroscopy (XPS) measurements were carried out with a K-Alpha spectrometer (Thermo-Scientific, Waltham, MA, USA). The spectra were collected with Al Kα radiation (1486.6 eV), monochromatized by a twin crystal monochromator, yielding a focused elliptical X-ray spot (ca. 0.314 mm^2) at 3 mA × 12 kV. Charge compensation was achieved with the system flood gun. Surface elemental composition was calculated from background-substracted peak areas by using Avantage software. The deconvolution of XPS spectra was done by least squares using Lorentzian-Gaussian (L/G = 30 %) functions.

Thermogravimetric analyses (TGA) of the prepared ligand with its copper complex were accomplished by using a PerkinElmer TGA 7 analyzer apparatus. Measurements were done by heating ca. 10–15 mg of the compounds from room temperature up to 950 °C at heating rates of 20 °C

min^{-1} under a N_2 atmosphere. The copper complex was electrochemically characterized by cyclic voltammetry at different scan rates by using a 301/10 Potentiostat/Galvanostat type PGZ 301-Voltalab 10 Radiometer with PC work-station and electrochemical interface IMT 301, with Volta Master 4 software. For this purpose, a standard three-electrode electrochemical cell of 10 mL was used. For this, the cyclic voltammetry of copper complex was maintained using glassy carbon (3 mm diameter) electrode, potentials are referred to the Hg/Hg_2Cl_2 saturated with KCl electrode, whereas a Pt wire was used as counter electrode. For these experiments, 10^{-3} M $Cu(L)_2{\cdot}2H_2O$ solutions, including 10^{-1} M tetra-n-butylammonium perchlorate (TBAP) as supporting electrolyte, were prepared in DMF and DMSO solvents. The voltammograms for DMSO solutions were recorded from –1.6 to +1.4 V, whereas those for DMF were registered between –1.4 and +1.4 V.

4. Catalytic activity of new ligand Cu-based complexes for catechol oxidation

The potential interest of the new ligand to prepare Cu-based catalysts was studied. Particularly, the activity of these catalysts for catechol oxidation was analyzed. The complexes were prepared in situ, by mixing 0.15 mL of a 2.10^{-3} mol/L solution of copper salts $CuX_y{\cdot}nH_2O$ (with X = Br^-, Cl^-, NO_3^-, CH_3COO^-, SO_4^{2-} and y = 1 or 2) with 0.15 mL of the ligand solution ($2{\cdot}10^{-3}$ mol/L).

These mixtures were then used for the oxidation of a 10^{-1} mol/L catechol solution. For this purpose, the absorbance of the resulting *o*-quinone oxidation product was followed over the time from 0 to 60 min at about 390 nm (Scheme 2). These measurements were carried out at 25 °C in the methanol solvent by using a UV-Vis. Spectrophotometer (UV PROB SHIMADZU 1700).

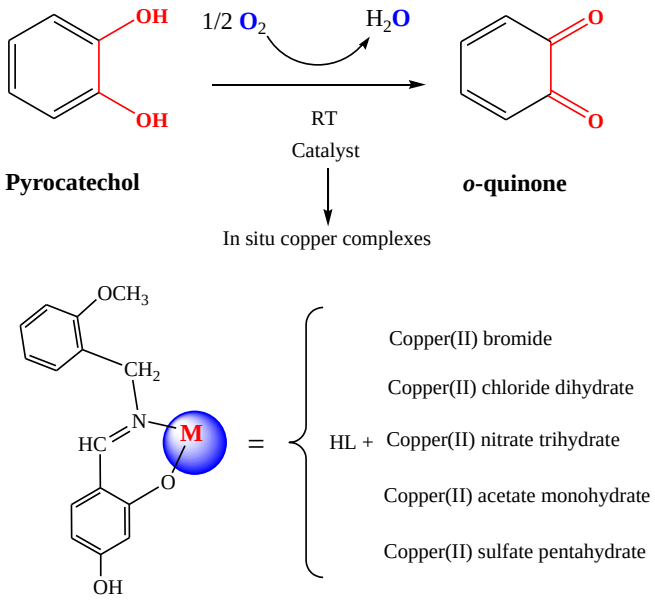

Scheme 2 – Oxidation reaction of catechol to *o*-quinone in the presence of the new copper complexes catalysts.

RESULTS AND DISCUSSION

1. Physico-chemical properties and molecular formula of the Bidentate Schiff Base ligand and its copper complex

The novel yellow powder of HL was easily synthesized by condensation reaction as can be seen in Scheme 1. From the chemical composition determined by elemental analysis it can be deduced that the molecular formula of the synthesized compound (HL) is $C_{15}H_{15}NO_3$.

On the other hand, the synthesized complex is intensively coloured, stable in air and moisture free solid. This compound is soluble in common organic solvents such as DMF, ACN, MeOH and DMSO. The elemental analysis indicates that the molecular formula of this copper complex, denoted as $[Cu(L)_2{\cdot}2H_2O]$, is $C_{30}H_{32}N_2O_8Cu$.

HL: FT-IR (KBr pellet, cm^{-1}): 3250–3650 (br, O-H, phenolic), 2820–3000 (w, C-H aliphatic and aromatic), 1644 (s, C=N), 1247 (m, C–O). ^1H NMR ($CDCl_3$, d (ppm)): 13.96 (s, 1H, –O–H), 9.95 (s, 1H, –O–H), 8.46 (s, 1H, H–C=N–)), 7.4–6.2 (m, phenyl-H), 4.70–4.65 and 3.88–3.84 (d, 2H, N–CH_2–), 2.54

(s, 3H, –CH_3). Anal. Calc. for $C_{15}H_{15}NO_3$: C 70.02; H 5.88; N 5.44; Found: C 69.59; H 5.54; N 5.66%.

$Cu(L)_2{\cdot}2H_2O$: FT-IR (KBr pellet, cm^{-1}): 3250–3650 (br, O–H, Water), 2820–3000 (w, C–H aliphatic), 1604 (s, C=N), 1213 (m, C–O), 600–500 (w, Cu–O), 500–400 (w, Cu–N). Anal. Calc. for $C_{30}H_{32}N_2O_8Cu$: C 58.86; H 5.27; N 4.58; Found: C 59.11; H 4.88; N 5.03 %.

2. Spectroscopic characterization

2.1. FT-IR spectroscopy

Figure 1 shows the FT-IR spectra of the synthesized ligand and its copper complex. In both cases, the FT-IR spectrum exhibits a characteristic broad band in the range 3250–3650 cm^{-1}, which can be assigned to O–H stretching (νO–H) and some weak absorption bands in the region 3000–2800 cm^{-1}, which may be attributed to aliphatic C–H stretching (νC–H).[28] Moreover, the band observed at 760 cm^{-1} is assigned to deformation vibrations of these aromatic C–H moieties, whereas those between 1050 and 1020 cm^{-1} may be related to the stretching vibration of the methoxy group (νC–O–C). On the other hand, the strong absorption band at about 1644 cm^{-1} may correspond to the stretching of the imine group (νC=N)[29] and the medium intensity band at 1247 cm^{-1} is ascribed to the phenolic νC–O stretching mode. Apart from these similarities, the spectrum of the complex showed some particularities. Thus, the azomethine stretching vibration in the ligand (νC=N) was shifted towards lower frequencies in the copper complex spectrum (observed at 1604 cm^{-1}). In addition, the νC–O stretching mode shifted to around 1213 cm^{-1}. These bathochromic shifts suggest the coordination of the ligand through its iminic nitrogen and phenolic oxygen atoms, respectively. This agreed with the new bands at ca. 400–500 cm^{-1} and 500–600 cm^{-1} assigned to Cu–N[30] and Cu–O[31] vibrations, respectively. All these IR features are in line with the molecular structures proposed in the Scheme 1, in which the ligand contains an imine group with the methoxybenzyl and meta-dihydroxybenzene substituents coming from the precursors.

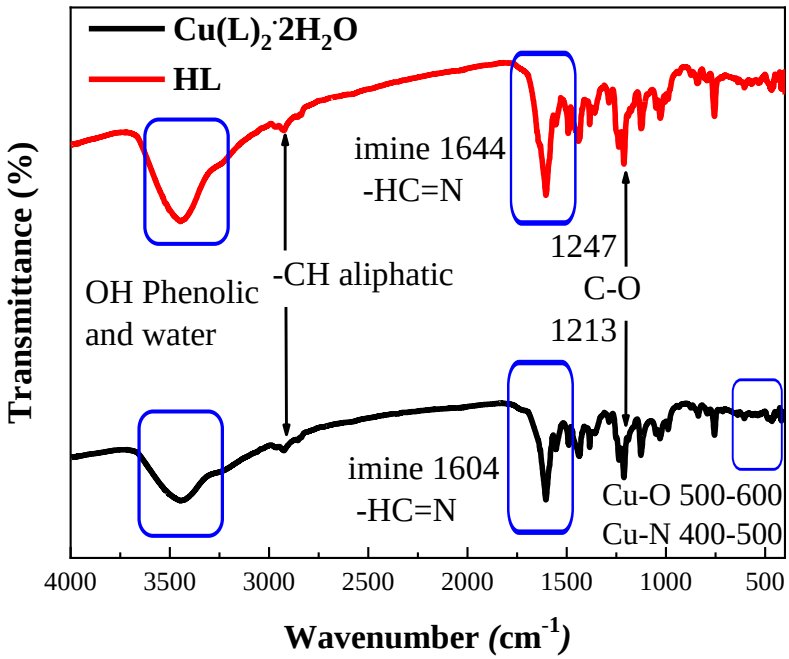

Fig. 1 – The FT-IR spectra of the ligand (HL) and its synthesized copper complex [$Cu(L)_2{\cdot}2H_2O$].

2.2. ^{1}HNMR spectroscopy

The ^{1}HNMR spectrum of the HL ligand is represented in Fig. 2. The spectrum exhibits resonances at δ = 13.96 and 9.95 ppm attributed to –OH phenolic-like protons. The highly observed deshielded is due to OH···N intra-molecular hydrogen bonding. Also, the Schiff base presents a singlet at 8.46 ppm, assigned to the proton in the azomethine (N=C–H) group.[32] Moreover, the ^{1}H NMR spectrum shows a multiplet between 6.2 and 7.4 ppm due to the protons of phenyl rings.[33] Furthermore, the peak seen between 4.70–4.65 ppm can be attributed to the hydrogens in the methylene groups adjacent to the azomethine

group (–CH_2–HC=N). Finally, the signal at 3.85 ppm can be related to the protons in the –CH_3 moiety.[34] All these features can be related to the proposed molecular structure shown in the inlet of the Fig. 2. Compared to the theoretical spectrum related to the protons of the amino group NH_2 of the 2-methoxybenzylamine reactant, the spectrum of the HL revealed the absence of the signal at 1.54 ppm confirmed the formation of the azomethine group.

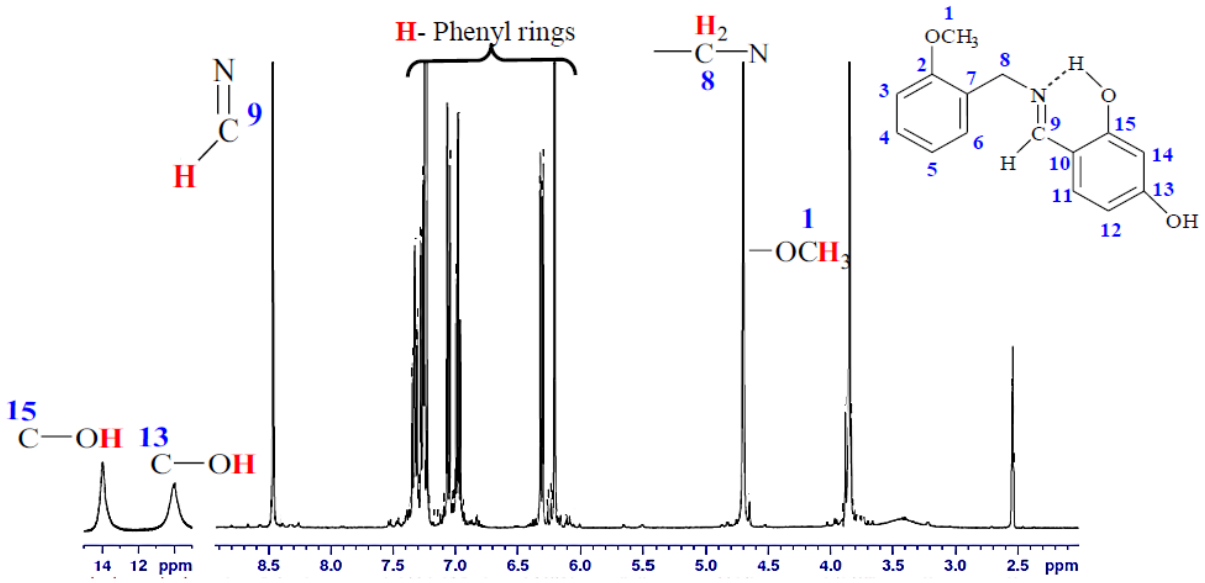

Fig. 2 – ^{1}HNMR spectrum of the Schiff base ligand (HL).

2.3. XPS characterization

X-ray photoelectron spectroscopy (XPS) was used to study the composition and local environment of the atoms in the synthesized compounds. Table 1 compiles the atomic composition of the synthesized ligand and its copper complex together with the predicted percentages deduced from the proposed molecular formula. As it can be observed, the determined surface atomic compositions as well as the C to N ratios of both substances are in quite good agreement with the predicted ones. This result suggests that the real composition of the synthesized compounds remarkably approaches that of the proposed $C_{15}H_{15}NO_3$ and $C_{30}H_{32}N_2O_8Cu$.

Table 1

Atomic surface composition and C to N ratios in the proposed (calculated from formulae) and real synthesized (XPS) ligand (HL) and copper complex ($Cu^{II}(L)_2{\cdot}2H_2O$)

		at. %				
		C	O	N	Cu	C/N
HL	$C_{15}H_{15}NO_3$	78.9	15.8	5.3	–	15.0
	XPS	82.6	12.7	4.8	–	17.4
$Cu^{II}(L)_2{\cdot}2H_2O$	$C_{30}H_{32}N_2O_8Cu$	73.2	19.5	4.9	2.4	15.0
	XPS	78.5	14.5	5.3	1.7	14.9

On the other hand, from the qualitative point of view, the C(1s) and O(1s) core-level spectra of the ligand and the complex were quite similar, and reflected the atomic bonding environments of carbon and oxygen species envisaged in the proposed structures of Scheme 1. Since these carbon and oxygen atomic environments of the synthesized substances were broadly consistent with those of the precursors, they were not considered to derive relevant conclusions. By

contrast, the nature of N species was expected to significantly change from the precursors to the ligand and complex as proposed in Scheme 1.

Figure 3A shows the N(1s) core-level X-ray photoelectron spectra of the ligand and its copper complex. In the case of the ligand, the spectrum can be deconvoluted into two main contributions. The bigger one centered at 401.2 eV has been assigned to C-N=C environment,[35,36] whereas the contribution shifted to 399.9 eV may be associated to a loss of electronic density around this N. This could be, for example, related to the formation of a H bond between this N and a neighboring OH group. Hence, the observation of these bands agrees with the formation of the shift base ligand proposed in the Scheme 1.

Respect to the nature of copper in the complex, Fig. 3B shows the Cu($2p^{3/2}$) and Cu($2p^{1/2}$) spin-orbit components of Cu2p photoelectrons, which display a split of ca. 19.5–19.7 eV and an intensity ratio of 0.51. The main Cu($2p^{3/2}$) contribution centered at 934.5 eV, together with the broad shake-up satellite between 938–946 eV are indicative features of Cu(II) species in the compound.[37-39]

This is in line with the shape and binding energy (571.2 eV) in the CuLMM Auger electron spectrum of the complex (Fig. 3C).[37] Consequently, XPS characterization confirms that copper exhibits +2 oxidation state in the synthesized complex ($Cu^{II}(L)_2{\cdot}2H_2O$).

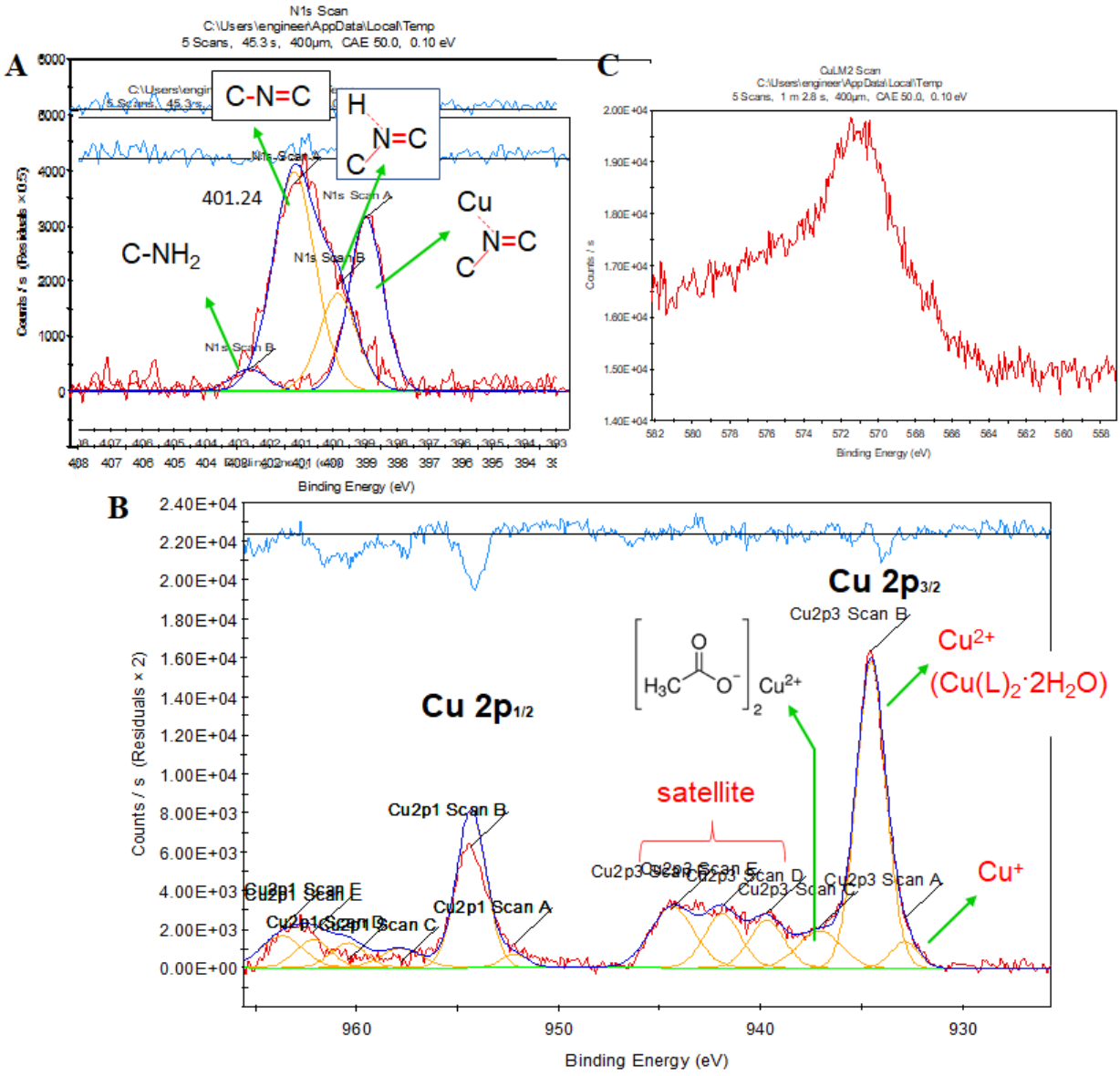

Fig. 3 – XPS spectra of (A) N(1s) core-level of the synthesized ligand and its copper complex; and (B) Cu(2p) core-level and (C) CuLMM Auger electron spectra of the copper complex.

Nevertheless, the small contribution in Cu($2p^{3/2}$) region at lower binding energies (932.9 eV) (Fig. 3B) could be related to some reduced species, *i.e.* Cu(I),[37,39] whereas the shoulder at ca. 936 eV might be associated to the presence of Cu(II) linked to atoms or a group of atoms with a higher-demanding electron density. This small contribution may be probably assigned to Cu(II) acetate, *i.e*. the copper precursor that might remain unreacted and present in the final product after the synthesis, what coincides with the low-intensity but clear band at 291.4 eV, attributed to acetate, observed in C(1s) spectrum of the complex. In agreement with a previous work,[38] hence, the main Cu($2p^{3/2}$) contribution shifted to lower binding energies respect to Cu(II) acetate precursor may be well explained by the fact that copper ions in the synthesized $Cu^{II}(L)_2{\cdot}2H_2O$ complex accept electrons from nitrogen atoms to form the coordinate bonds between Cu and N.

Supporting the formation of a coordinate bond, a significant change in the N(1s) spectrum of the ligand was observed after complexation (Fig. 3A). Particularly, a main symmetric contribution appears centered at 398.9 eV. In line with the previous hypothesis about the formation of a H bond, the shift of the N(1s) spectrum further towards even lower binding energies may be related to the formation of a new bond of N (in C-N=C) with a higher electron demanding specie, like a metallic ion. Hence, the observed shift in the N(1s) spectrum seems to confirm the formation of N-Cu(II) bonds in the complex, as proposed in the Scheme 1.

2.4. UV-Vis. spectroscopy

The electronic spectrum of the HL was recorded using freshly prepared solutions of 10^{-5} M in different solvents, what permitted to study some interesting properties of this compound. As shown in Fig. 4A, the Schiff base ligand showed relatively intense absorption bands in the near ultraviolet region. The stronger and higher energy bands in the 270–340 nm region were attributed to the π-π* transition of the benzene ring chromophore, while the weaker and less energetic band at 340–440 nm were assigned to the n-π* transition involving the promotion of the lone pair electron of azomethine nitrogen atom to the anti-bonding π orbital associated with the azomethine group.[40]

Interestingly, Fig. 4A shows that the position (energy) of the absorption maxima of the Schiff base ligand (summarized in Table 2) changed depending on the nature of the solvent. This remarkable change of UV-Vis. absorption characteristics induced by using different solvents can be considered a solvatochromism effect associated to their different polarities.[41] The observed shifting towards higher energies in solvents of higher polarity (like CH_3OH and ACN) was indicative of a polar ground state and non-polar excited state,[42] whereas a shift towards longer wavelengths is observed in less polar solvents, such as DCM and THF.[43,44] Such a hypsochromic behavior in solvents of higher polarity has already been observed and seems to be a general trend for salicylaldiminato Schiff base complexes.[45,46]

Respect to the copper complex, Fig. 4B shows the UV-Vis. spectrum recorded in 10^{-5} M solutions prepared with different solvents. It has to be stressed that the band at around 300 nm is not present, while the red shift of the n to π* transition of the C=N group suggests the coordination of the nitrogen atoms of the azomethine groups to the metal center, in line with a more extended conjugated system after deprotonation of phenolic hydrogens, and the formation of phenoxides in the complex.[47] The observed UV-Vis. bands and shifts are in agreement with the proposed molecular structure of the ligand and the complex proposed in the Scheme 1.

Table 2

UV-Vis. properties of the ligand (HL) and its copper complex [$Cu^{II}(L)_2{\cdot}2H_2O$] in different solvents (c = 10^{-5} mol/L)

Solvent	λ_1 (nm)		λ_2 (nm)		λ_3 (nm)	
	HL	**$Cu^{II}(L)_2{\cdot}2H_2O$**	**HL**	**$Cu^{II}(L)_2{\cdot}2H_2O$**	**HL**	**$Cu^{II}(L)_2{\cdot}2H_2O$**
DCM	275	283	310	–	388	351
THF	276	285	311	–	–	354
ACN	275	287	304	–	385	350
DMF	280	289	309	–	385	352
DMSO	282	292	308	–	385	352
MeOH	–	290	304	–	372	350

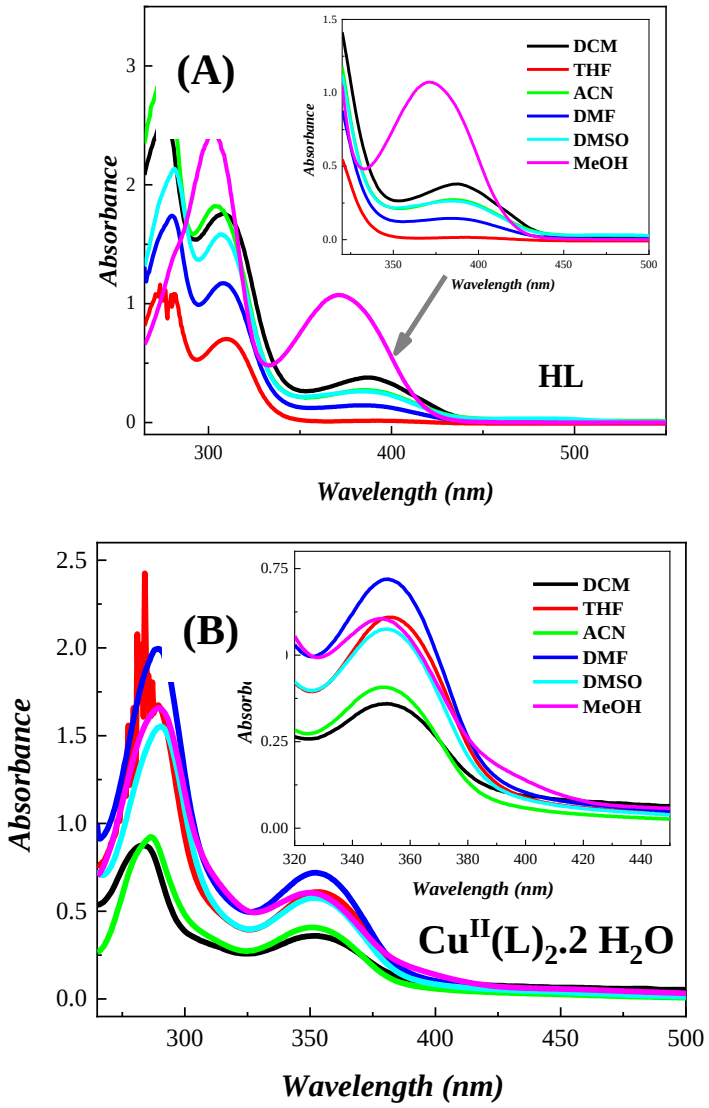

Fig. 4 – UV-Vis. absorption spectra of (A) the ligand (HL) and (B) its copper complex $[Cu^{II}(L)_2 \cdot 2H_2O]$ in different solvents ($c = 10^{-5}$ mol/l).

3. Thermal behavior

The TG/DTG curves of the ligand and its copper complex are shown in Fig. 5. The thermal analyses were performed in a nitrogen atmosphere with a heating rate of 20 °C/min over a temperature range of 25–950 °C/min. As can be observed, both compounds show a gradual weight loss indicating their thermal decomposition by fragmentation with the increasing temperature. Particularly, the TG curve of the bidentate Schiff base ligand (HL) undergoes three main decomposition stages, with the corresponding DTG peaks centered at about 200, 230, and 506 °C, respectively. The first weight loss of ca. 46.94% (calculated weight loss = 47.14%) that can be assigned to the loss of the 2-methoxybenzyl groups (CH_2–Ph–OCH_3). Next, the second decomposition step from about 300 to 380 °C, accounting for a weight loss of 10.97% (calculated weight loss = 10.52%), could be ascribed to the loss of the azomethine group (CHN). Finally, the third step of decomposition occurring between 380–950 °C shows a weight loss of 42.91% (calculated weight loss = 42.41%) and may be due to the loss of the remaining part of the ligand (Dihydroxyphenyl).

On the other hand, the copper complex was also thermally decomposed in three successive steps (Fig. 5B**)**. The first step occurring within 25–150 °C can be ascribed to the loss of two hydration molecules with an estimated mass loss 6.09% (calculated mass loss = 5.88 %). The second step of decomposition, with a weight loss of 19.51% (calculated mass loss = 19.79 %), is attributed to the

removal of the methoxybenzyl group. The last one between 490–950 °C and with a weight loss of 60.97% (calculated mass loss = 61.33%) may be due to the loss of the remaining part of the both ligands ($C_{22}H_{19}N_2O_4$) yielding the copper oxide (CuO) as the final decomposition product.[48]

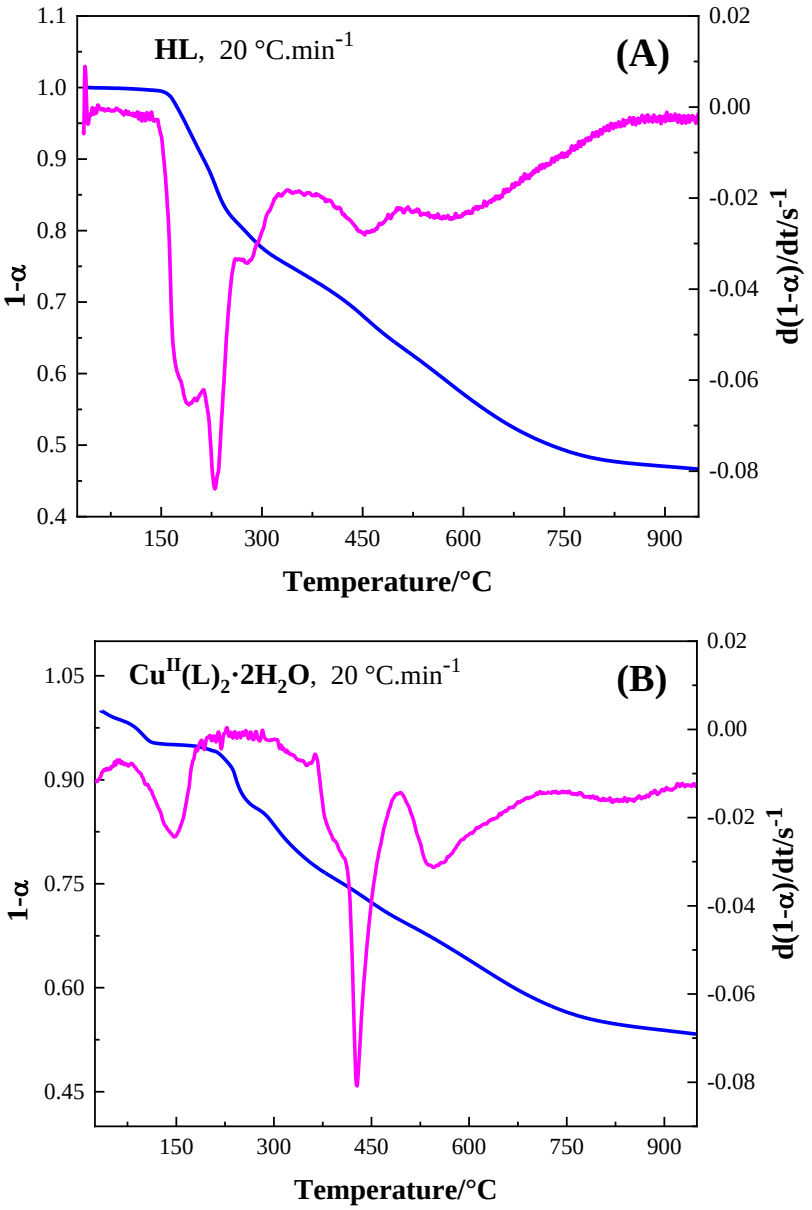

Fig. 5 – TG and DTG curves for (A) HL and (B) $Cu^{II}(L)_2{\cdot}2H_2O$ (heating rate = 20 °C/min).

4. Relevant features and potential applications

4.1. Naked-eye chemosensor of metal ions

The capability and selectivity of HL for complexing divalent and trivalent metal ions was studied in different solvents. Such a complexation capacity presents great interest for sensor applications. In this sense, the ability of the ligand to act as a sensor towards various metal ions, such as Al^{3+}, Ba^{2+}, Ca^{2+}, Cd^{2+}, Co^{2+}, Cr^{3+}, Cu^{2+}, Fe^{2+}, Fe^{3+}, K^+, Li^+, Mn^{2+}, Na^+, Ni^{2+}, Pb^{2+} and Zn^{2+} was examined in MeOH and ACN solvents through the color observation (naked-eye detection) and UV spectroscopy (Fig. 6).

As observed by the naked eye (Fig. 6A), the change from colorless to green-, blue- and yellow-colored solutions indicate that the ligand exhibited a distinctive selectivity to Cu^{2+}, Co^{2+} and Fe^{3+} ions, respectively, in ACN. Thus, the spectroscopic analysis revealed that the free ligand HL shows two main absorption bands centered at 304 and 385 nm in this solvent. With the addition of 1.0 equiv Cu^{2+} to

probe HL, a new broad absorption band centered at 465 nm was observed, while the band at 304 nm maintained its position and that at 385 nm rather disappeared. On the other hand, the addition of 1.0 equiv Co^{2+} caused a new broad absorption band, with two maxima centered at 580 and 682 nm, while the bands of the ligand exhibited a blue shift to 298 and 340 nm, respectively. Based on the fundamentals of UV spectroscopy,[49] these spectroscopic changes reflect that new intramolecular charge transfer (ICT) processes are taken place upon complexation with these metallic species.

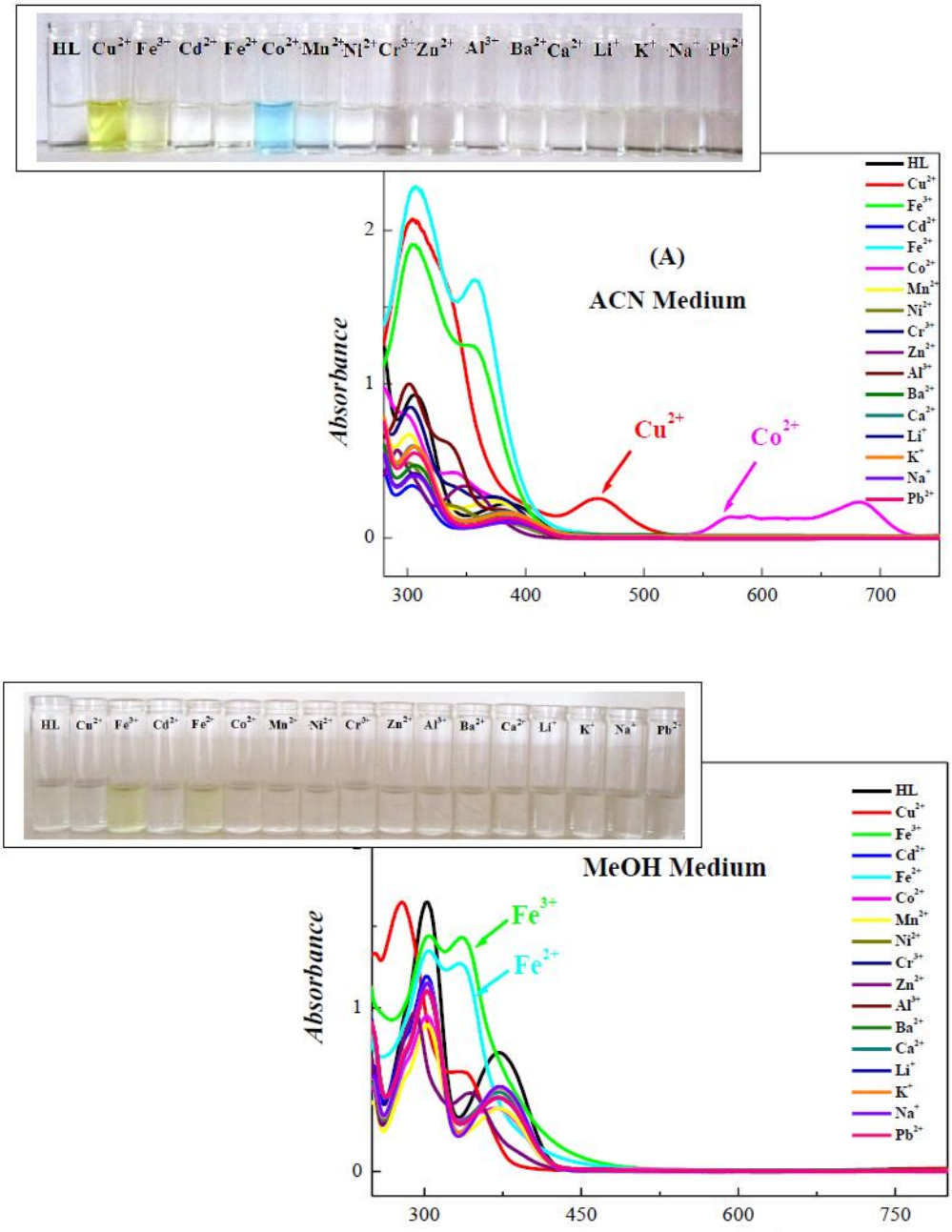

Fig. 6 – Photographs and UV spectra of different solutions of HL (10^{-4}M) before and after addition of various metal ions (1 equiv) in ACN (**A**) and MeOH (**B**) solvents.

In contrast, and except for Fe^{2+}, Fe^{3+} and Al^{3+} which present a minor response, the addition of other metal ions to the HL probe produced no significant color change and, consequently, a negligible absorption change. It is well known that the binding ability depends on the size, charge and electron configuration of the metal ion and ligand. The obtained results, thus, suggest that these features belonging to Cu^{2+} and Co^{2+} and the ligand are suitable for each other to form metal complexes.

The main practical implication of such an extraordinary selectivity to Cu^{2+} and Co^{2+} is that HL may be considered an interesting probe for naked-eye detection of these ions.

On the other hand, only Fe^{2+} and Fe^{3+} showed a color change from colorless to yellowish in methanol solvent (Fig. 6B). Spectroscopically, the two main UV absorption bands of the HL ligand were found centered at 302 and 372 nm in this solvent. From UV-spectra comparison it can be observed that the addition of 1.0 equiv Fe^{2+} and Fe^{3+} to HL probe causes a significant blue shift of its second band to 336 nm for both ions. By contrast, the addition of the other metal ions produced no relevant effects in the spectroscopic features of the ligand, except for Cu^{2+}. In this case, the whole spectrum was shifted towards lower wavelengths, but the absorbance at 336 nm was considerably lower than in the case of Fe species, probably explaining the lesser noticeable color change by the naked eye. Again, such an exclusive response towards Fe species in MeOH reflects the interesting selectivity of the HL ligand for sensing applications.

The sensing capability of HL towards Cu^{2+}, as one of the most interesting examples, was further studied at different concentrations in ACN. As observed in Fig. 7, upon addition of an increasing amount of copper ion into the solution with HL sensor, the intensity of the absorption band centered at 460 nm gradually increases. This coincides with a progressive change in color from almost transparent to stronger yellow (inset of Fig. 7). Interestingly, the increment in band absorbance and the color change finished when only 0.5 equiv Cu^{2+} was added. This result suggests that the HL chemosensor coordinates with Cu^{2+} with a 2:1 stoichiometry. So, this behavior is consistent with the formation of a stable complex of the kind $[(L)_2$-$Cu^{2+}]$ upon detecting Cu^{2+} in ACN solution.

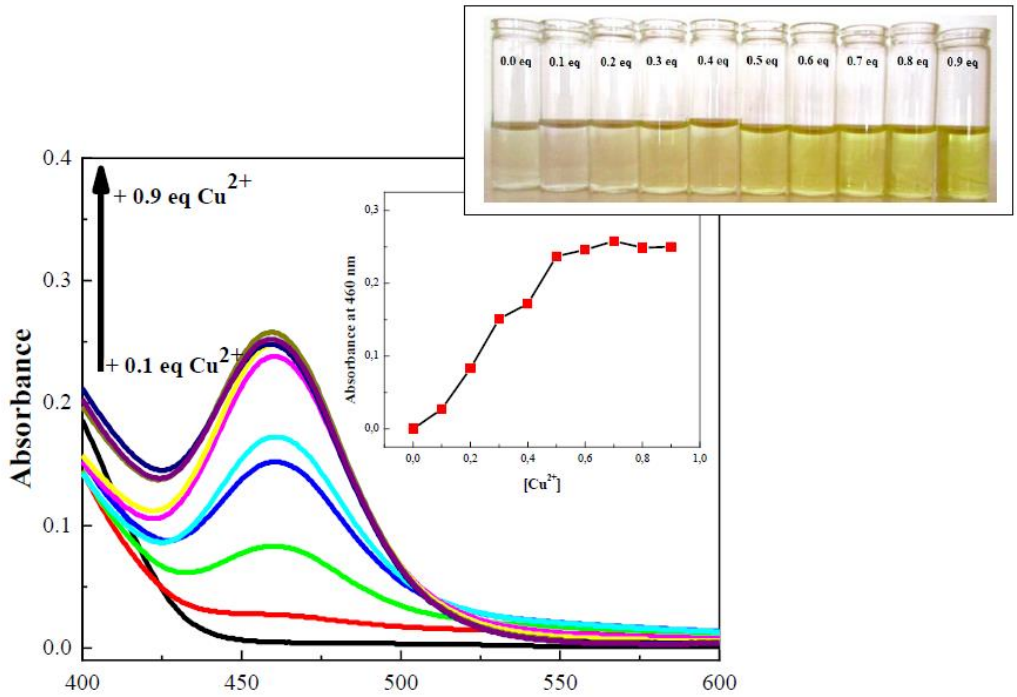

Fig. 7 – UV-Vis. absorption spectra of HL in ACN solution with gradual addition of Cu^{2+}. Inset 1: changes in absorbance at 460 nm; Inset 2: changes in color.

4.2. Electrochemical behavior of the copper complex

The electrochemical behavior of the copper complex $Cu^{II}(L)_2 \cdot 2H_2O$ was investigated by cyclic voltammetry in DMSO and DMF solvents containing 0.1 M TBAP.

As observed in Fig. 8A, the wide-potential-range voltammogram of the complex in DMSO presents various quasi-reversible processes, in the medium potential range, followed by some irreversible oxidations above +0.5 V.

Particularly, two redox processes can be discerned in the medium potential range, being the reduction counterparts more clearly discernable than the oxidation ones. At more negative potentials, the well-defined reduction peak centered at $Ep(C_1)$ = –0.87 V, with its oxidation counterpart

centered at ca. $Ep(A_1)$ = –0.70 V may be assigned to the reduction and oxidation of Cu(II)/Cu(I) in the complex.[50] In addition, the voltammogram also displays a clear cathodic peak and a broad low-intensity anodic counterpart at $Ep(C_2)$ = –0.49 V and $Ep(A_2)$ = –0.04 V, respectively, probably related to the Cu(III)/Cu(II) redox process in the complex. These redox processes were better discerned within their corresponding delimited potential ranges (Figs. 8B and 8C). The found wide peak potential separations, all far from 60 mV, are consistent with rather quasi-reversible one electron redox processes.[51] On the other hand, the irreversible anodic peaks at +0.40, +0.77 and above +1.0 V may be related to the oxidation of the Schiff base ligand, as previously reported for this type of complexes.[52]

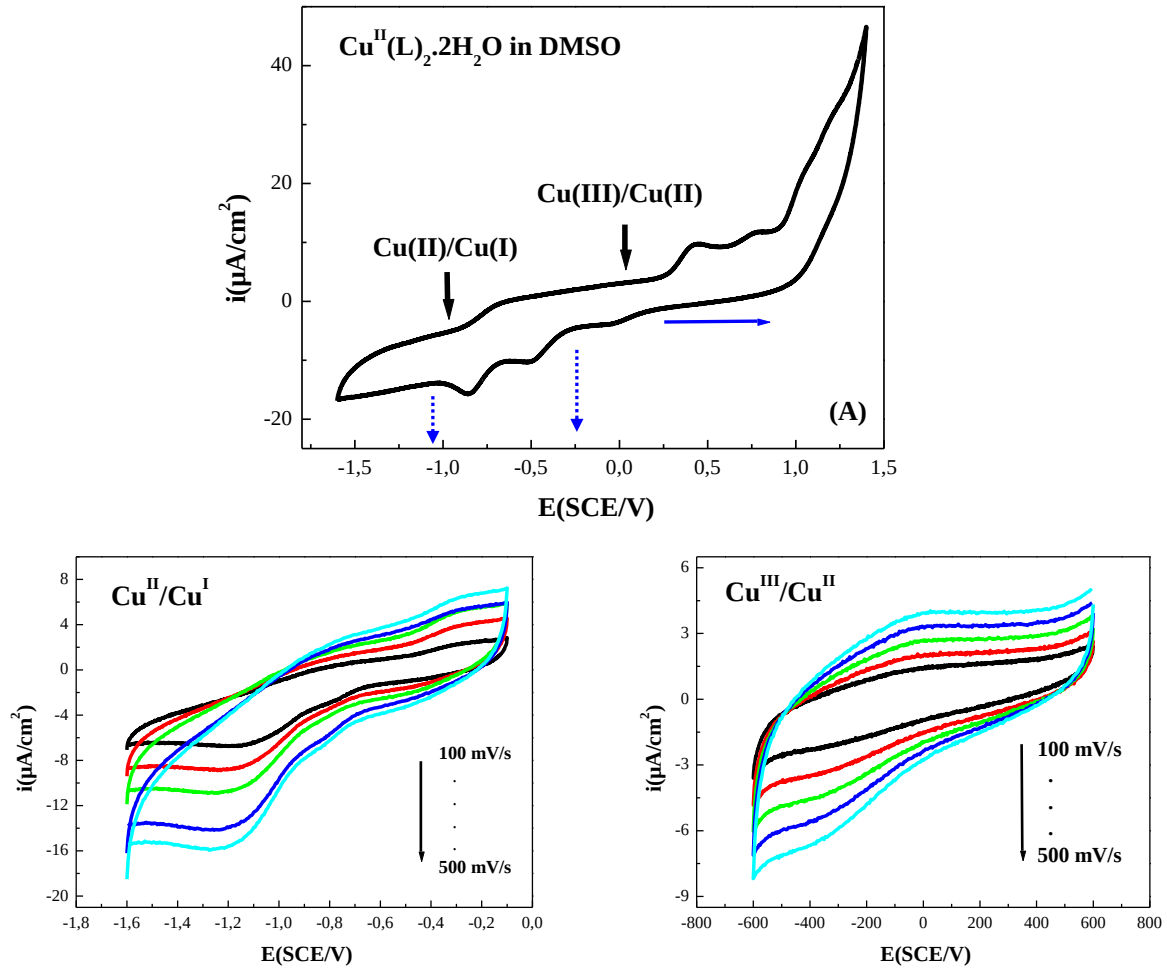

Fig. 8 – Cyclic voltammograms of the synthesized copper complex (10^{-3} M) recorded on a GC-electrode in 0.1 M TBAP/DMSO withing the whole stability potential window at 100 mV/s (A); and at different scan rates (100, 200, 300, 400, 500 mV·s^{-1}) withing the particular potential ranges of the assigned Cu^{II}/Cu^{I} (B) and Cu^{III}/Cu^{II} (C) redox systems.

The voltammetric curves obtained for the copper complex in DMF are presented in Fig. 9A. In general, the electrochemical behavior of the complex observed in this solvent was remarkably similar to that previously obtained for DMSO. Nevertheless, a shift in the peak potentials was observed and some differences were significant because of the different solvent. Thus, in DMF solution the Cu(II)/Cu(I) couple is shifted towards lower potentials ($Ep(C_1)$ = –1.00 V; and $Ep(A_1)$ = – 0.85 V), and while the reduction of Cu(II) is considerably much more intense than in DMSO, the oxidation of Cu(I) is practically indiscernible. By contrast, in DMF the Cu(III)/Cu(II) process was slightly shifted towards more positive potentials ($Ep(C_2)$ = – 0.30 V; and $Ep(A_2)$ = 0.00 V) and the oxidation counterpart was more noticeable than the cathodic one. Moreover, the increase in oxidation current from 0.35 V and a clear anodic peak observed at 1.15 V was attributed to the oxidation of Schiff base ligand.[53]

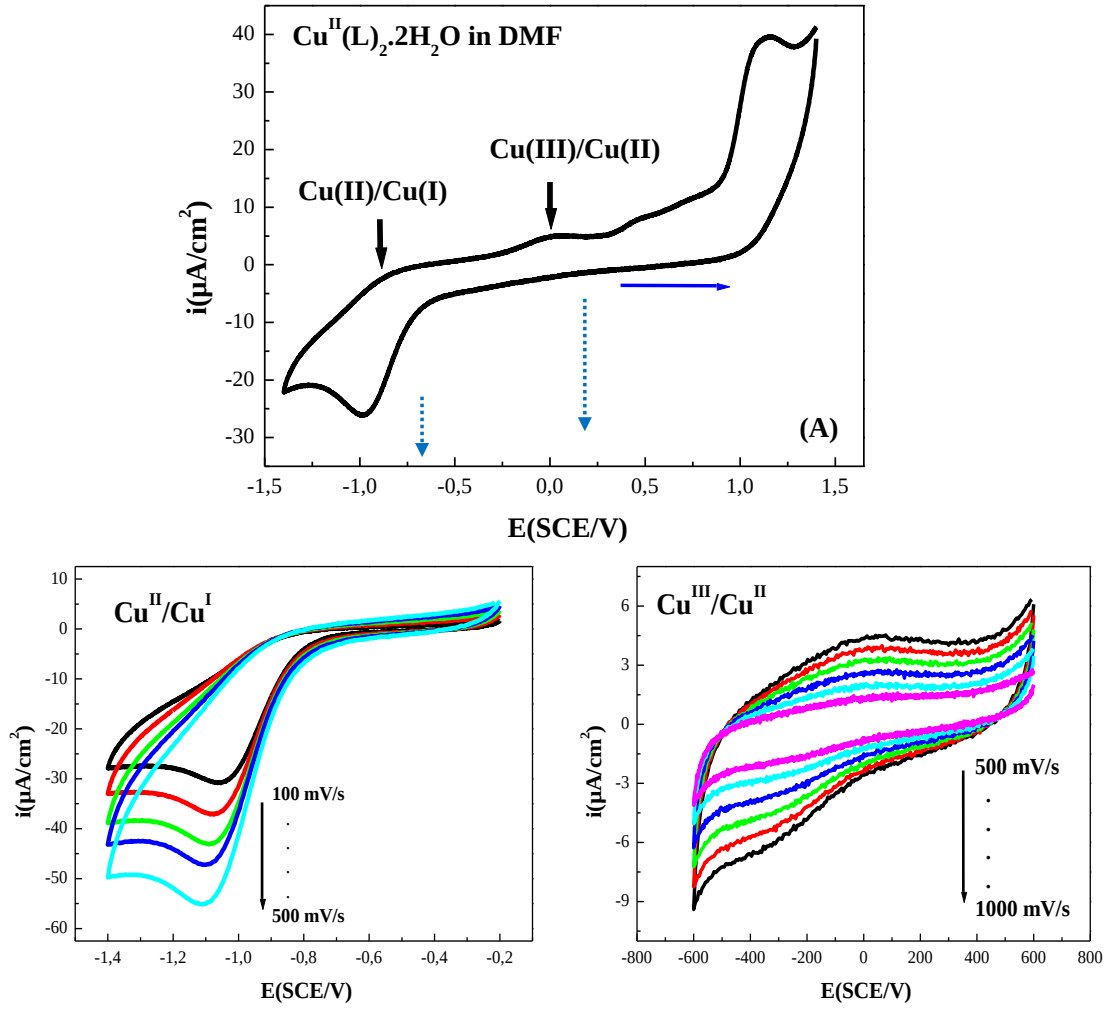

Fig. 9 – Cyclic voltammograms of the synthesized copper complex (10^{-3} M) recorded on a GC-electrode in 0.1 M TBAP/DMF withing the whole stability potential window at 100 mV/s (A); and at different scan rates (100, 200, 300, 400, 500 mV.s^{-1}) withing the specific potential ranges of the assigned Cu^{II}/Cu^{I} (B) and Cu^{III}/Cu^{II} (C) redox systems.

To further study the electrochemical behavior of the copper complex in both solvents, the influence of the scan rate on the voltammetric response was analyzed withing the specific potential ranges of the assigned Cu^{II}/Cu^{I} and Cu^{III}/Cu^{II} redox systems (Figs. 8B–C and 9B–C). On the one hand, and independently of the solvent and scan rate, it can be generally observed that the i_{pa}/i_{pc} ratios are systematically lower than unity; and that the oxidation of Cu(I) shows considerably lower currents than the other electrochemical processes, especially in DMF solvent. These findings suggest that the oxidation processes in the complex are somehow hampered compared to the reduction ones.

On the other hand, except in the case of Cu(I) oxidation in DMF, the figures generally evidence a gradual increase in the anodic and cathodic peak currents (i_{pa}, i_{pc}) and a progressive peak potential separation ($\Delta Ep = Epa - Epc$) with the increasing scan rate. In particular, a good linear relationship was found between the peak currents and the scan rate, what reflects that the electrochemical process involves a surface-controlled process,[51] whereas the increasing peaks potential separation (ΔEp) points out that the reversibility of these processes decreases with the scan rate.

4.3. Catalytic activity studies

o-Benzenediol, also known as pyrocatechol, was used as substrate to explore the biomimicking catecholase activity of copper complexes that where prepared *in situ* from diverse copper(II) salts and the new ligand HL. The capability of these complexes to catalyze the oxidation of pyrocatechol was spectrophotometrically studied by following the absorbance band appearance of

the corresponding oxidized product, 1,2-Benzoquinone (*o*-quinone) over time. For this kinetic study, the absorbance was quantified at 390 nm (wavelength of the band maximum). It is noteworthy to mention that a blank experiment was previously tested, so that the spectrum obtained for pyrocatechol alone, without the studied copper complexes, practically showed no absorbance chance as a function of time.

The kinetics of catechol oxidation was then studied in the presence of distinct copper complexes. Fig. 10 shows the evolution of the maximum absorbance as a function of time for the different complexes coming from salts with the anions Br^-, Cl^-, NO_3^-, CH_3COO^- and SO_4^{2-}. The obtained results indicate that the copper complexes formed from bromide and nitrate salts present significantly better performance for pyrocatechol oxidation, especially for the case of $CuBr_2$ salt.

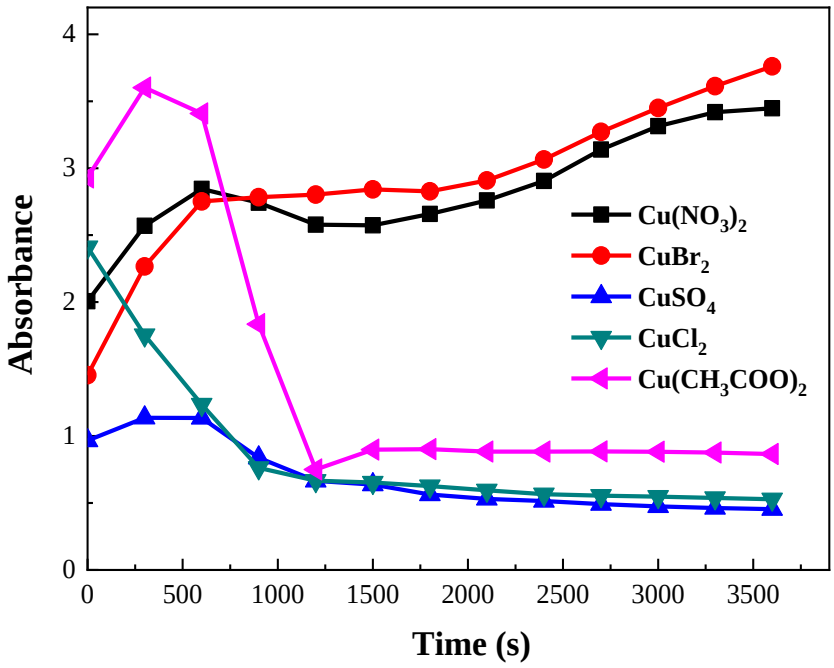

Fig. 10 – Evolution of the absorbance to follow the catechol oxidation (o-quinone formation) in the presence of copper complexes, prepared from distinct copper salts, formed *in situ* with HL in MeOH medium.

Table 3

Oxidation rate of catechol oxidation (μmol L^{-1} min^{-1}) in MeOH by using different ligand to metal ion ratios (L/M) (best result obtained with metal salts: $CuBr_2$ and $Cu(NO_3)_2$)

	(L/M: 1/1)	**(L/M: 2/1)**	**(L/M: 1/2)**
$Cu(NO_3)_2$	1.5	–	0.0128
$CuBr_2$	2.4	–	0.00625

4.3.1. Effect of HL concentration

The effect of HL concentration, during the synthesis process, on the catalytic activity of the new copper complexes was studied. To do this, complexes obtained from solutions with different ligand to metal ion ratios (L/M: 1/1, 2/1 and 1/2) were tested in methanol solution under ambient conditions. On the other hand, because of their better performance, only the complexes obtained from $CuBr_2$ and $Cu(NO_3)_2$ salts were considered.

The monitored absorbance of *o*-quinone as a function of the different complexes is displayed in Fig. 11. The obtained results indicate that the different L/M combinations affect the catalytic activity of the complexes. Thus, the L/M: 1/1 combination has been found the best catalytic condition for this reaction. These results can be explained probably by the influence of coordination environment, such as the geometry imposed by the ligand on the metal ion complex, together with the characteristics of the steric effect of ligand.[54,55]

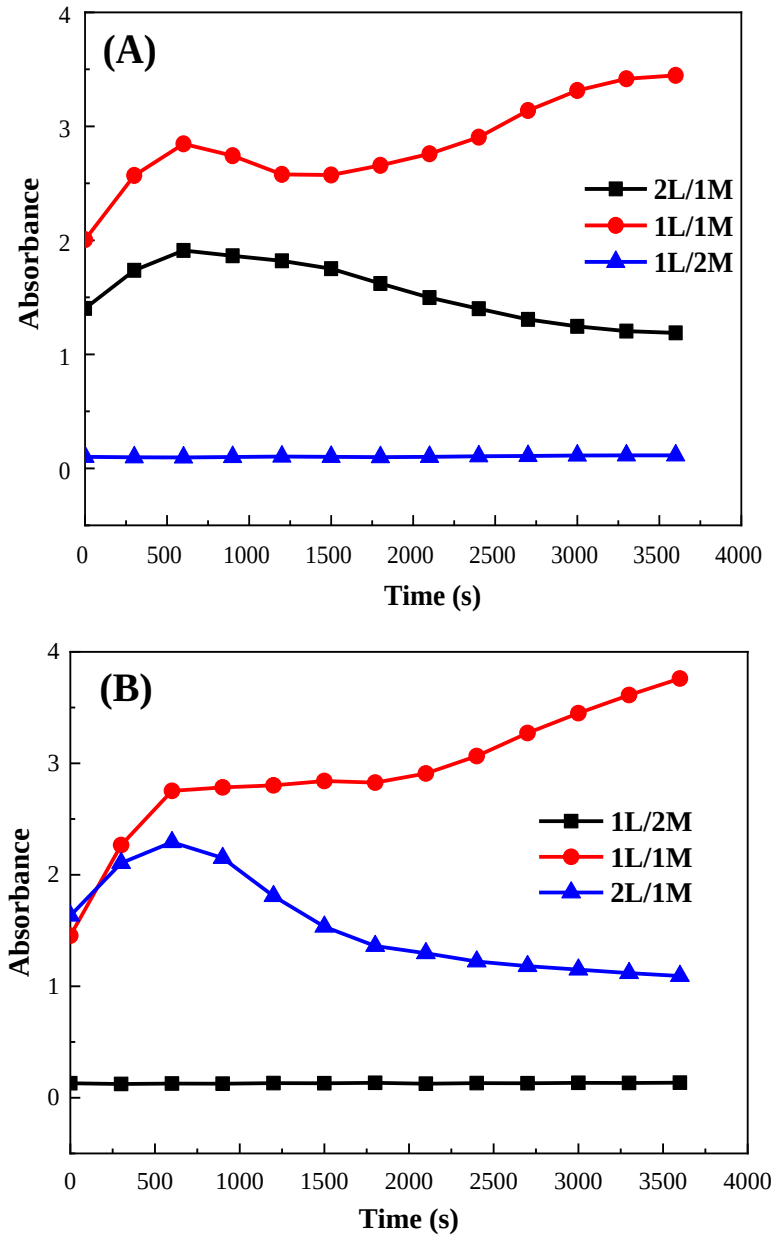

Fig. 11 – Catechol oxidation in methanol in presence of formed L-Copper complexes with different concentration prepared from (A) NO_3^- and (B) Br-based salts

4.3.2. Solvent effect

Finally, the oxidation reaction of catechol was also studied under the same experimental conditions with the best catalyst but in distinct solvent media. For this purpose, ACN and DMF, besides MeOH, were used as solvents. Figure 12 and Table 4 show the influence of the solvent in the evolution o-quinone absorbance as well as the calculated oxidation constant rates, respectively.

The obtained data point out a remarkable effect of the solvent polarity in the catalytic activity of the new complexes. Particularly, the reaction in MeOH, which is a protic and polar solvent, seems to work significantly better than in the other two aprotic solvents (ACN and DMF), which cannot provide oxidation rates higher than 2.4 μmol L^{-1} min^{-1}. These results suggest that solvation of the copper complexes with these aprotic solvents slows their catalytic activity for this oxidation reaction. These results are in agreement with those previously obtained in the literature,[56–58] and can be explained by the fact that, although copper cations can be also solvated by the electronegative pole of aprotic solvents, this solvation is weaker than that produced by a hydrogen bond in protic ones. Then, a weaker solvation results in a lower or moderate reactivity.

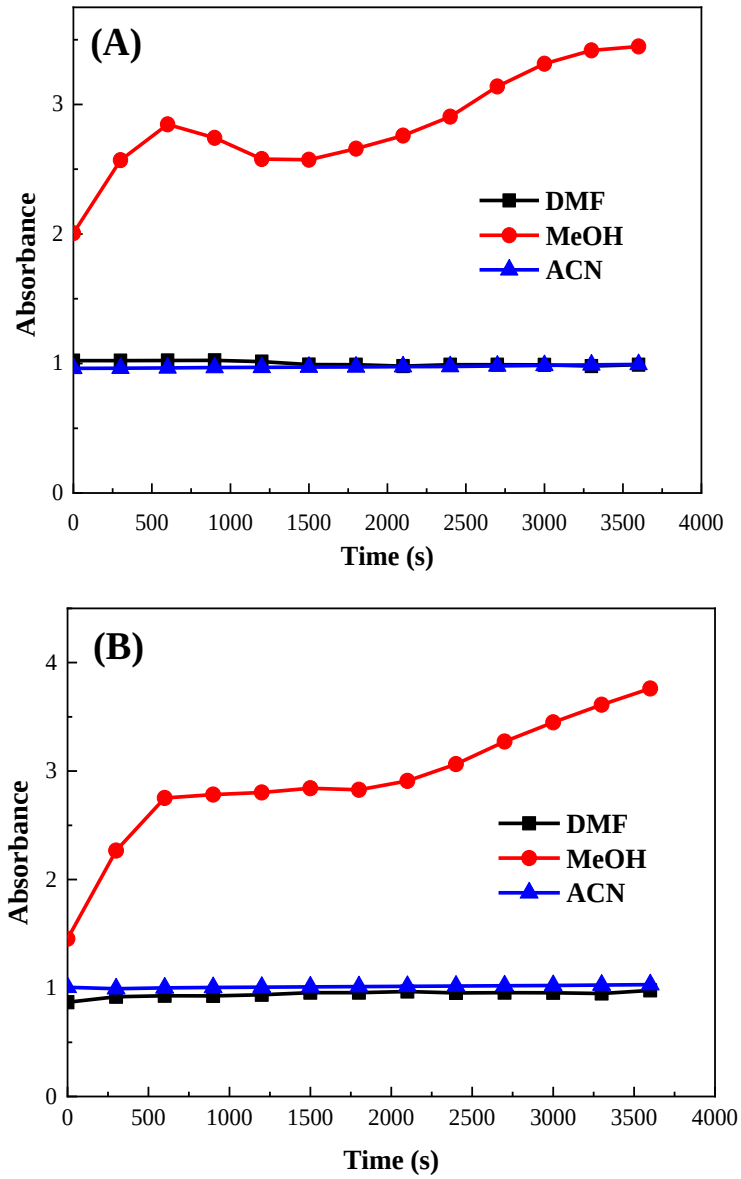

Fig. 12 – Evolution of the absorbance at about 390 nm to follow the catechol oxidation (o-quinone formation) in different solvents in the presence of copper complexes prepared from (A) NO_3^- and (B) Br-based salts with a L/M = 1/1 ratio.

Table 4

Rate constants of catechol oxidation (μmol L^{-1} min^{-1}) in different solvents catalyzed by the copper complexes prepared from $CuBr_2$ and $Cu(NO_3)_2$ salts by using a L/M = 1/1 ratio

	MeOH	**ACN**	**DMF**
$Cu(NO_3)_2$	**1.5**	0.032	–
$CuBr_2$	**2.4**	0.0965	0.027

CONCLUSIONS

In this present paper, a novel asymmetric N,O-bidentate Schiff base ligand (HL) and its $[Cu^{II}(L)_2 \cdot 2H_2O]$ copper complex were synthesized and fully characterized by various techniques revealing their structures.

The main results are summarized as follows:

The prepared Schiff base ligand presents the molecular formula $C_{15}H_{15}NO_3$ with an imine bond linked to methoxybenzyl and meta-dihydroxybenzene substituents; whereas that of its copper complex is $C_{30}H_{32}N_2O_8Cu$ in the form of $Cu^{II}(L)_2 \cdot 2H_2O$, as deduced from CHN-EA, TG/DTG thermogravimetry

and various spectroscopic investigations, like FT-IR, ^{1}HNMR, XPS and UV-Vis.

For the X-ray photoelectron spectroscopy (XPS), the determined surface atomic compositions as well as the C to N ratios of both proposed $C_{15}H_{15}NO_3$ and $C_{30}H_{32}N_2O_8Cu$ compounds are in quite good agreement with the predicted ones. This result suggests that the metal is coordinated to the ligand through its iminic nitrogen and phenolic oxygen atoms and validates the structures of these compounds.

The electrochemical behavior of the copper complex $Cu^{II}(L)_2 \cdot 2H_2O$ was investigated by cyclic voltammetry in DMSO and DMF solvents containing 0.1 MTBAP and resulting obtained voltammograms indicate well-defined redox systems of Cu(II)/Cu(I) and Cu(III)/Cu(II). Moreover, this complex has been found electrochemically stable and electroactive in organic media, what is of potential interest for various electrochemical processes and applications.

The obtained results further reveal that the synthesized ligand has an extraordinary selectivity for detecting Cu^{2+}, Co^{2+} Fe^{2+} and Fe^{3+} species in different organic solvents. It is proved that this novel ligand could potentially serve as a powerful naked-eye molecular chemosensor for detecting these ions.

For the catalytic study, the ligand was testified and inspected for its catecholase activities at ambient conditions on the oxidation of catechol to the o-quinones via formation of a mononuclear copper species. These species were generated *in situ*. Some parameters influencing the catalytic activity were tested such as, the effect of copper salt used, the effect of concentration and the effect of the solvent. The rate constants of catechol oxidation were also calculated.

The obtained results demonstrate that the new *in situ* copper complexes prepared with bromide and nitrate copper(II) salts and with L/M: 1/1 ratio exhibit an interesting catecholase-like activity in methanol medium.

Acknowledgements. The authors thank the Algerian Ministry of Higher Education and Scientific Research (MESRS) and the Director General for Scientific Research and Technological Development (DGRSDT) for the financial support.

REFERENCES

1. H. Keypour, M. Shayesteh, M. Rezaeivala, F. Chalabian, Y. Elerman and O. Buyukgungor, *J. Mol. Struct.*, **2013**, *1032*, 62–68. https://doi.org/10.1016/j.molstruc.2012.07.056
2. C. Anitha, C. D. Sheela, P. Tharmaraj and S. Sumathi, *Spectrochim. Acta Part A*, **2012**, *96*, 493–500. https://doi.org/10.1016/j.saa.2012.05.053
3. D. Aggoun, Z. Messasma, B. Bouzerafa, R. Berenguer, E. Morallon, Y. Ouennoughi and A. Ourari, J. Mol. Struct., **2021**, *1231*, 129923. https://doi.org/10.1016/j.molstruc.2021.129923
4. B. Shaabani, A.A. Khandar, M. Dusek, M. Pojarova and F. Mahmoudi, *Inorg. Chim. Acta*, **2013**, *394*, 563–568. https://doi.org/10.1016/j.ica.2012.08.027.
5. (a) D. Aggoun, D. López, M. Fernández García, B. Bouzerafa, Y. Ouennoughi, A. Bezza, H. Bezzi and A. Ourari, *Rev. Roum. Chim.*, **2022**, *67*, 271–282. DOI: 10.33224/rrch.2022.67.4-5.06; (b) H. Keypour, M. Shayesteh, M. Rezaeivala, F. Chalabian and L. Valencia, *Spectrochim. Acta Part A*, **2013**, *101*, 59–66. https://doi.org/10.1016/j.saa.2012.09.048.
6. K. Mohammadi, S. S. Azad and A. Amoozegar, *Spectrochim. Acta Part A*, **2015**, *146*, 221–227. https://doi.org/10.1016/j.saa.2015.02.069
7. S. Rayati, M. Koliaei, F. Ashouri, S. Mohebbi, A. Wojtczak and A. Kozakiewicz, *Appl. Catal. A-Gen*., **2008**, *346*, 65–71. https://doi.org/10.1016/j.apcata.2008.05.016
8. O. A. M. Ali, S. M. El-Medani, D. A. Ahmed and D. A. Nassar, *Spectrochim. Acta Part A*, **2015**, *144*, 99–106. https://doi.org/10.1016/j.saa.2015.02.078
9. E. E. Shehata, M. S. Masoud, E. A. Khalil and A. M. Abdel-Gaber, *J. Mol. Liq.*, **2014**, *194*, 149–158. https://doi.org/10.1016/j.molliq.2013.10.003
10. M. T. H. Tarafder, K. T. Jin, K. A. Crouse, A. M. Ali, B. M. Yamin and H.-K. Fun, *Polyhedron*, **2002**, *21*, 2547–2554. https://doi.org/10.1016/S0277-5387(02)01188-9
11. M. S. Nair, D. Arish and R. S. Joseyphus, *J. Saudi Chem. Soc.*, **2012,** *16*, 83–88. https://doi.org/10.1016/j.jscs.2010.11.002
12. Z. Messasma, D. Aggoun, S. Houchi, A. Ourari, Y. Ouennoughi, F. Keffous and R. Mahdadi, *J. Mol. Struct.*, **2021**, *1228*, 129463. https://doi.org/10.1016/j.molstruc.2020.129463
13. S. M. Emam, I. E. T. El Sayed and H. M. R. Hathout, *J. Mol. Struct*., **2017**, *1146*, 600–619. https://doi.org/10.1016/ j.molstruc.2017.06.006
14. M. Behpour, S. M. Ghoreishi, N. Soltani and M. Salavati-Niasari, *Corros. Sci*., **2009**, *51*, 1073–1082. https://doi.org/ 10.1016/j.corsci.2009.02.011
15. P. Nigam, S. Mohan, S. Kundu and R. Prakash, *Talanta*, **2009**, *77*, 1426–1431. https://doi.org/10.1016/j.talanta.2008.09.026
16. G. Venkatachalam and R. Ramesh, *Inorg. Chem. Commun.*, **2006**, *9*, 703–707. https://doi.org/10.1016/j.inoche.2006.04.012
17. S. Dalapati, M. A. Alam, S. Jana, S. Karmakar and N. Guchhait, *Spectrochim. Acta Part A*, **2013**, *102*, 314–318. https://doi.org/10.1016/j.saa.2012.10.038
18. A. Ourari, A. Alouache, D. Aggoun, R. R. Rosas and E. Morallon, *Int. J. Electrochem. Sci.*, **2018**, *13*, 5589-5602. https://doi.org/10.20964/2018.06.39
19. A. Ourari, I. Bougossa, S. Bouacida, D. Aggoun, R. Ruiz-Rosas, E. Morallon and H. Merazig, *J. Iran. Chem. Soc*., **2017**, *14*, 703–715. https://doi.org/10.1007/s13738-016-1022-8
20. (a) R. Egekenze, Y. Gultneh and R. Butcher, *Polyhedron*, **2018**, *144*, 198–209. https://doi.org/10.1016/j.poly.2018.01.008; (b) M. Mureşeanu, V. Parvulescu, G. Petcu, S. Nastase, T. D. Pasatoiu and M. Andruh, *Rev. Roum. Chim.*, **2023**, *68*, 153–164. DOI: 10.33224/rrch.2023.68.3-4.05; (c) Q. Cao, M. Diefenbach, C. Maguire, V. Krewald, M. J. Muldoon and U. Hintermair, *Chem. Sci.*, **2024**, *15*, 3104–3115. https://doi.org/10.1039/D3SC05516G.
21. A. Şenol, E. A. Akanbong, M. Sudagidan and A. K. Devrim, *Rev. Roum. Chim*., **2021**, *66*, 701–711. DOI: 10.33224/rrch.2021.66.8-9.02.

22. M. Shabbir, Z. Akhter, I. Ahmad, S. Ahmed, V. McKee, and B. Mirza, *Polyhedron*, **2017**, *124*, 117–124. https://doi.org/10.1016/j.poly.2016.12.039
23. S.K. Dhar, Inorg. Chim. Acta, 240 (1995) 609–614. https://doi.org/10.1016/0020-1693(95)04589-9
24. (a) N.vH. Boukoucha, Z. Messasma, D. Aggoun, Y. Ouennoughi, C. Bensouici, M.vFernandez-García, D. Lopez, M. Guelfi, F. Marchetti, G. Bresciani and Z. Chorfi, *J. Mol. Struct.*, **2025**, *1319*, 139505. https://doi.org/10.1016/j.molstruc.2024.139505; (b) Z. Chorfi, Z. Messasma, D. Aggoun, S. Houchi, C. Bensouici, M. Fernández-Garcîa, D. López, M.S. Abd El-Maksoud, F. Setifi, A. Ourari and Y. Ouennoughi, *Ind. J. Chem. Tech*., **2024**, *31*, 105–124. DOI: 10.56042/ijct.v31i1.7607.
25. S. Kr Dey, A. Mukherjee, *New J. Chem*., **2014**, *38*, 4985–4995. https://doi.org/10.1039/C4NJ00715H
26. M. Mitra, P. Raghavaiah and R. Ghosh, *New J. Chem*., **2015**, *39*, 200–205. https://doi.org/10.1039/C4NJ01587H
27. D. Aggoun, A. Ourari, R. Ruiz-Rosas and E. Morallon, *Spectrochim. Acta Part A*, **2017,** *184*, 299–307. https://doi.org/10.1016/j.saa.2017.05.022
28. R. Takjoo, A. Akbari, S. Y. Ebrahimipour, H. Amiri Rrudbari and G. Brunò, *C. R. Chim*., **2014**, *17*, 1144–1153. https://doi.org/10.1016/j.crci.2014.01.009
29. B. Shafaatian, A. Soleymanpour, N. K. Oskouei, B. Notash and S. A. Rezvani, *Spectrochim. Acta Part A*, **2014**, *128*, 363–369. https://doi.org/10.1016/j.saa.2014.02.179
30. S. Y. Ebrahimipour, I. Sheikhshoaie, A. Crochet, M. Khaleghi and K. M. Fromm, *J. Mol. Struct*., **2014**, *1072*, 267–276. https://doi.org/10.1016/j.molstruc.2014.05.024
31. A. Ourari, D. Aggoun and L. Ouahab, *Inorg. Chem. Commun*., **2013**, 118–124. https://doi.org/10.1016/j.inoche.2013.04.002
32. C. Demetgül, M. Karakaplan, S. Serın and M. Diğrak, *J. Coord. Chem*., **2009**, *62*, 3544–3551. https://doi.org/10.1080/00958970903082192
33. C. Demetgül, D. Deletıoğlu, F. Karaca, S. Yalçinkaya, M. Tımur and S. Serın, *J. Coord. Chem*., **2010**, *63*, 2181–2191. https://doi.org/10.1080/00958972.2010.496852
34. R. Vafazadeh and M. Kashfi, *Bull. Kor. Chem. Soc*., **2007**, *28*, 1227–1230. https://doi.org/10.5012/bkcs.2007.28.7.1227
35. E. Murugan, S. Santhosh Kumar, K. M. Reshna and S. Govindaraju, *J. Mater. Sci.*, **2019**, *54*, 5294–5310. https://doi.org/10.1007/s10853-018-3184-5
36. Y. Zhou, L. Zhang and W. Wang, *Nature Commun*., **2019,** *10*, 506. DOI: 10.1038/s41467-019-08454-0
37. M. C. Biesinger, *Surf. Interface Anal.*, **2017**, *49*, 1325–1334. https://doi.org/10.1002/sia.6239
38. M. Jiang, Y. Tuo and M. Cai, *J. Porous Mat.* **2020**, *27*, 1039–1049. https://doi.org/10.1007/s10934-020-00880-6
39. M. Swadzba-Kwásny, L. Chancelier, S. Ng, H.G. Manyar, C. Hardacre and P. Nockemann, *Dalton Trans*., **2012**, *41*, 19–227. https://doi.org/10.1039/c1dt11578b
40. M. Salehi, M. Amirnasr, S. Meghdadi, K. Mereiter, H. R. Bijanzadeh and A. Khaleghian, *Polyhedron*, *81* 90–97. https://doi.org/10.1016/j.poly.2014.05.049
41. B. Shafaatian, M. Hashemibagha, B. Notash and S. A. Rezvani, *J. Organomet. Chem*., **2015,** *791*,51–57. https://doi.org/10.1016/j.jorganchem.2015.05.037
42. S. D. Cummings and R. Eisenberg, *J. Am. Chem. Soc*., **1996,** *118*, 1949–1960. https://doi.org/10.1021/ja951345y
43. A. Trujillo, M. Fuentealba, D. Carrillo, C. Manzur, I. Ledoux-Rak, J.-R. Hamon and J.-Y. Saillard, *Inorg. Chem.*, **2010**, *49*, 2750–2764. https://doi.org/10.1021/ic902126a
44. S. Celedon, V. Dorcet, T. Roisnel, A. Singh, I. Ledoux-Rak, J.-R. Hamon, D. Carrillo and C. Manzur, *Eur. J. Inorg. Chem.*, **2014**, 4984–4993. https://doi.org/10.1002/ejic.201402469
45. P. G. Lacroix, *Eur. J. Inorg. Chem*., **2001**, 339–348. https://doi.org/10.1002/1099-0682(200102)2001
46. J. Cisterna, V. Dorcet, C. Manzur, I. Ledoux-Rak, J.-R. Hamon and D. Carrillo, *Inorg. Chim. Acta*, **2015**, *430*, 82–90. https://doi.org/10.1016/j.ica.2015.02.030
47. S. Abolfaz, Hosseini-Yazdi, A. Mirzaahmadi, P. Samadzadeh-Aghdam, A. A. Khandar, G. Mahmoudi, W. S. Kassel and William G. Dougherty, *Inorg. Chim. Acta*, **2014**, *414*, 115–120. https://doi.org/10.1016/j.ica.2014.01.039
48. H. P. Ebrahimi, J. S. Hadi, Z. A. Abdulnabi and Z. Bolandnazar, *Spectrochim. Acta Part A*, **2014**, 485–492. https://doi.org/10.1016/j.saa.2013.08.044
49. H. Gunzler and A. Williams, "Handbook of Analytical Techniques", WILEY-VCH Verlag GmbH, D-69469 Weinheim (Federal Republic of Germany), 2001. DOI:10.1002/9783527618323
50. A. Ourari, W. Derafa and D. Aggoun, *RSC Adv*., **2015,** *5*, 82894–82905. https://doi.org/10.1039/C5RA10819E
51. A. J. Bard and L. R. Faulkner, "Electrochemical Methods: Fundamentals and Applications", 2nd edition, John Wiley& Sons: New York, NY, USA, 2001.
52. P. Gili, M. G. M. Reyes, P. M. Zarza, I. L. F. Machado, M. F. C. Guedes da Silva, M. A. N. D. A. Lemos and A. J. L. Pombeiro, *Inorg. Chim. Acta*, **1996,** *244*, 25–36. https://doi.org/10.1016/0020-1693(95)04756-5
53. B. Bouzerafa, D. Aggoun, Y. Ouennoughi, A. Ourari, R. Ruiz-Rosas, E. Morallon and M. S. Mubarak, *J. Mol. Struct*., **2017**, *1142*, 48–57. https://doi.org/10.1016/j.molstruc.2017.04.029
54. R. El Ati, A. Takfaoui, M. El Kodadi, R. Touzani, Yousfi, F. A. Almalki and T. Ben Hadda, *Mater. Today: Proc*., **2019**, *13*. 1229–1237. https://doi.org/10.1016/j.matpr.2019.04.092
55. S. Thabti, A. Djedouani, S. Rahmouni, R. Touzani, A. Bendaas, H. Mousser and A. Mousser, *J. Mol. Struct*., **2015**, *1102*, 295–301. https://doi.org/10.1016/j.molstruc.2015.08.071
56. A. Mouadili, A. Attayibat, S. El Kadiri, S. Radi and R. Touzani, *Appl. Cata. A Gen.*, **2013**, *454*, 93–99. https://doi.org/10.1016/j.apcata.2013.01.011
57. K. S. Banu, M. Mukherjee, A. Guha, S. Bhattacharya, E. Zangrando and D. Das, *Polyhedron*, **2012**, *45*, 245–254. https://doi.org/10.1016/j.poly.2012.06.087
58. A. Djedouani, F. Abrigach, M. Khoutoul, A. Mohamadou, A. Bendaas, A. Oussaid and R. Touzani, *Orient. J. Chem.*, **2015**, *31*, 97–105. http://dx.doi.org/10.13005/ojc/310110